Rapid atmospheric CO_2 changes associated with the 8,200-years-B.P. cooling event

Friederike Wagner*†, Bent Aaby‡, and Henk Visscher*

*Department of Botanical Palaeoecology, Laboratory of Palaeobotany and Palynology, Utrecht University, Budapestlaan 4, 3584 CD, Utrecht, The Netherlands; and ‡Botanical Institute, Department of Ecology, Evolution and Diversity, University of Copenhagen, Øster Farimagsgade 2D, 1353 Copenhagen K, Denmark

Communicated by David L. Dilcher, University of Florida, Gainesville, FL, July 15, 2002 (received for review April 20, 2002)

By applying the inverse relation between numbers of leaf stomata and atmospheric CO_2 concentration, stomatal frequency analysis of fossil birch leaves from lake deposits in Denmark reveals a century-scale CO_2 change during the prominent Holocene cooling event that occurred in the North Atlantic region between 8,400 and 8,100 years B.P. In contrast to conventional CO_2 reconstructions based on ice cores from Antarctica, quantification of the stomatal frequency signal corroborates a distinctive temperature–CO_2 correlation. Results indicate a global CO_2 decline of ≈25 ppm by volume over ≈300 years. This reduction is in harmony with observed and modeled lowering of North Atlantic sea-surface temperatures associated with a short-term weakening of thermohaline circulation.

Estimates of Holocene atmospheric CO_2 concentrations strongly rely on CO_2 measured in air extracted from Antarctic ice cores. Records for the past millennium indicate significantly reduced CO_2 levels from A.D. 1550 to 1800, which are temporally related to the historical Little Ice Age climate deterioration (1, 2). By contrast, Antarctic ice-core data do not clearly support a temperature–CO_2 correlation during the eight earlier short-term cooling pulses that punctuated Holocene climatic conditions in the North Atlantic region with a periodicity of ≈1,500 years (3). Only the so-called 8.2-ka-B.P. cooling event has been associated with a long-term, modestly declining CO_2 trend recognized in the Taylor Dome record (2). This most prominent century-scale instability of Holocene climate is reflected as a negative $\delta^{18}O$ excursion in Greenland ice cores (4, 5) as well as in a variety of marine and terrestrial proxy records indicative of pronounced modifications of regional temperature and/or precipitation regimes in the North Atlantic region (3, 4, 6–11). The instability is related to a brief episode of massive release of meltwater associated with the final demise of the Laurentian ice sheet (12).

The conventional iced-based concept of relatively stabilized CO_2 concentrations during the greater part of the Holocene is challenged increasingly by stomatal frequency analysis of fossil leaves (13–15). Species of C_3 plants are often characterized by a plastic phenotype capable of consistent adjustment of numbers of leaf stomata in response to changes in ambient CO_2 concentration (16–18). Identification of a CO_2-sensitive gene involved in stomatal development in *Arabidopsis thaliana* demonstrates the genetic control of the response (19). As a corollary of this responsiveness, stomatal frequency analysis of fossil leaves enables the detection and quantification of atmospheric CO_2 changes at different time scales (14, 17–25). High-resolution analysis of tree leaves buried in Lateglacial and Holocene peat and lake deposits suggests temporal correlation between global CO_2 dynamics and Northern Hemisphere temperature. In Europe and North America, reconstructed CO_2 fluctuations (14, 15, 20) appear to parallel well documented $\delta^{18}O$ and chrinomid-based temperature changes associated with the Younger Dryas stadial and the Preboreal Oscillation, the first of the Holocene climatic instabilities occurring at ≈11,000 calendar years B.P. (26). Both Younger Dryas and Preboreal Oscillation are not apparent in the CO_2 record of Antarctic ice (2, 27), which may be due to generally low temporal resolution of Lateglacial and early Holocene CO_2 data from Antarctica.

To corroborate the concept of a coupling between recurrent Holocene cooling pulses and CO_2 fluctuations, we document stomatal frequency data that constrain timing and magnitude of CO_2 shifts associated with the prominent 8.2-ka-B.P. cooling event. We analyzed leaves of European tree birches (*Betula pubescens* and *Betula pendula*) preserved in cores of gyttja deposits from Lake Lille Gribsø, North of Copenhagen, Denmark (55°58′43′′N; 12°18′52′′E). Well preserved leaf remains occur continually through an interval corresponding to the period between ≈8,700 and ≈6,800 calendar years B.P. Temporal control is provided by a series of six accelerator mass spectrometry ^{14}C chronologies measured on single leaves (Table 1).

Stomatal frequency can be expressed in terms of stomatal density and stomatal index (SI): SI = (stomatal density/[stomatal density + epidermal cell density]) × 100. In contrast to stomatal density, SI reflects stomatal frequency independently of variation in epidermal cell size related to light intensity, temperature, or nutrient and water availability. In angiosperm leaves, therefore, mean SI is the more sensitive parameter for detecting stomatal frequency responses to changing CO_2 levels (28, 29). Effects of variation within and between leaves can be eliminated by using large data sets (17, 18, 28). Leaves of *B. pendula* and *B. pubescens* display essentially similar SI patterns and can be treated therefore as a single category in stomatal frequency analysis (18). There is sufficient evidence from field studies and experiments that CO_2-induced trends in mean SI for *Betula* leaves are not disturbed significantly by environmental factors other than CO_2 (30, 31).

Standardized, computer-aided determination of stomatal parameters on leaf cuticles was performed on a Leica Quantimet 500C/500+ image-analysis system. Measured parameters include stomatal density and epidermal cell density (including guard cells). Counting areas are restricted to stomata-bearing alveoles. Calculated SIs are mean values for up to seven leaves per data point. Seven digital images (field area, 0.035 mm^2) per leaf were analyzed (standard deviations are constant after seven counts). We used the rate of historical CO_2 responsiveness of the European tree birches (Fig. 1) to quantify early Holocene SI-based CO_2 levels. Our approach of inferring an unknown value of a quantitative variable (CO_2/x_0) from the quantitative response of a single taxon (SI_{birch}/y) meets the basic requirements for a classical linear regression, which allows a better performance at the extremes and with slight extrapolation (32–34).

The reconstructed CO_2 record shows a fluctuating pattern (Fig. 2). Inferred CO_2 minima with averages of ≈275 ppm by volume (ppmv) occur at ≈8,680 years B.P. and between ≈8,430 and ≈8,040 years B.P.; prominent maxima with values of 300–325 ppmv occur at ≈8,640 years B.P. and between ≈7,920 and

Abbreviations: ka, thousand years; ppmv, ppm by volume.

†To whom reprint requests should be addressed. E-mail: r.wagner@bio.uu.nl.

GEOLOGY

Table 1. Leaf-bearing and accelerator mass spectrometry ^{14}C-dated horizons in Lake Lille Gribsø, Denmark

Sample depth	Mean SI ± 1σ	Mean CO_2 ± 1σ	^{14}C date code	^{14}C age B.P.	Calendar years B.P. range at 1σ
485.5	11.0 ± 1.1	292 ± 16	—	—	—
490	10.8 ± 1.0	295 ± 15	AAR-5216	6200 ± 55	7104–7011
492.5	10.7 ± 1.2	296 ± 18	—	—	—
495	10.1 ± 1.2	305 ± 17	AAR-5215	6350 ± 100	7341–7205
502	9.4 ± 1.0	314 ± 14	—	—	—
504	10.6 ± 1.3	298 ± 18	—	—	—
506	9.6 ± 0.9	312 ± 13	AAR-5214	6840 ± 40	7692–7613
514	8.6 ± 0.8	326 ± 11	—	—	—
516	10.9 ± 1.0	293 ± 14	—	—	—
518	—	—	AAR-5213	7010 ± 55	7868–7787
524	10.3 ± 1.1	302 ± 17	—	—	—
526	11.4 ± 0.9	287 ± 13	—	—	—
528	—	—	AAR-4841	7475 ± 50	8345–8284
535	12.4 ± 1.6	271 ± 23	—	—	—
536	11.7 ± 1.0	281 ± 14	—	—	—
541	12.2 ± 0.8	275 ± 12	—	—	—
543	—	—	AAR-4843	7640 ± 55	8454–8372
544	12.2 ± 1.8	274 ± 27	—	—	—
549	10.3 ± 1.1	301 ± 14	—	—	—
553	9.8 ± 0.8	309 ± 11	—	—	—
554	12.1 ± 1.6	275 ± 23	—	—	—

Sample depth in cm below sediment surface; mean SI values ± 1σ of analyzed leaf material per horizon; mean atmospheric CO_2 concentration ± 1σ (ppmv) calculated according to historical training set (Fig. 1); laboratory code for accelerator mass spectrometry ^{14}C dates; uncalibrated ^{14}C ages ± 1σ; and calibrated calendar-age range at 1σ. Calibrations were performed with CALIB 4.3 HTTM version (www.calib.org).

≈7,270 years B.P. The series of low CO_2 concentrations around 8,300 years B.P. follow a declining trend of ≈25 ppmv within a time interval of <100 years. This interval ends with a return to

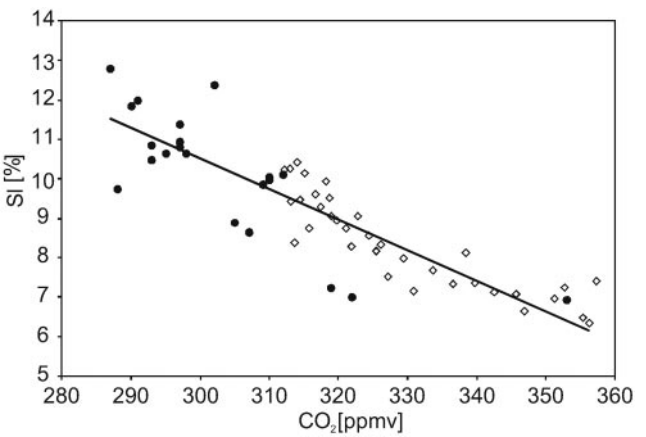

Fig. 1. Historical response of SI for European tree birches (*B. pendula* and *B. pubescens*) to global atmospheric CO_2 increase from 287 to 356 ppmv. The training set includes mean SI values for herbarium material (●) collected in The Netherlands and Denmark in the period 1843–1995 and leaf remains from living peat (◇) in The Netherlands, formed in the period 1952–1995 (17). Historical CO_2 concentrations of 315–356 ppmv are mean spring-season values from Mauna Loa monitoring (http://cdiac.esd.ornl.gov/ndps/ndp001.html), and concentrations of 287–315 ppmv are representative values derived from shallow Antarctic ice cores (http://cdiac.esd.ornl.gov/trends/co2/siple.htm). For analytical method, see text. Regression statistics: $n = 63$; slope = −0.0846. Goodness-of-fit linear model: $R^2 = 0.78$, $R^2_{adj} = 0.78$. Analysis of variance results: $F(1–62) = 225.11$ ($P = 0.000$). Statistical analyses were performed with SPSS 8 for Windows (Chicago). *B. pendula* and *B. pubescens* display significantly similar SI patterns and can be treated therefore as a single category in stomatal frequency analysis. Species-specific regression statistics: *B. pubescens*: slope = −0.0871; goodness-of-fit linear model: $R^2 = 0.63$, $R^2_{adj} = 0.60$; *B. pendula*: slope = −0.0724; goodness-of-fit linear model: $R^2 = 0.80$, $R^2_{adj} = 0.79$. Trend lines are not given in the figure.

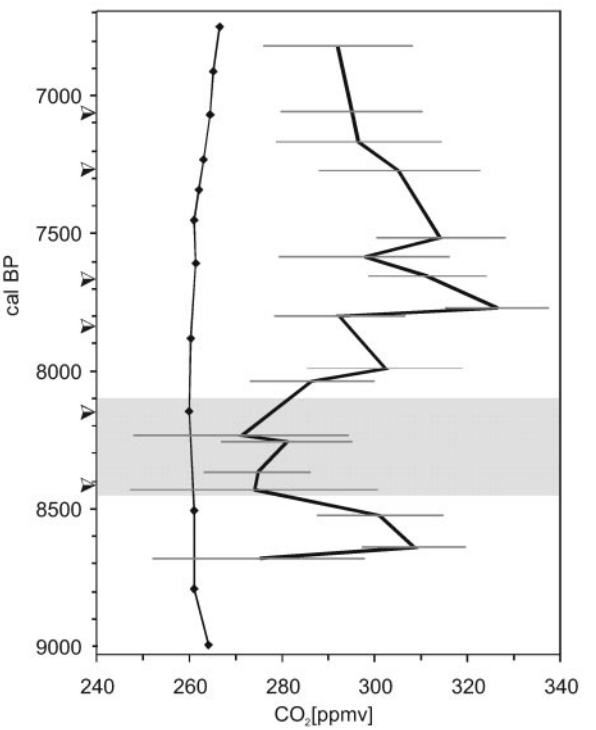

Fig. 2. Reconstructed CO_2 concentrations for the time interval between ≈8,700 and ≈6,800 calendar years B.P. based on CO_2 extracted from air in Antarctic ice of Taylor Dome (left curve; ref. 2; raw data available via www.ngdc.noaa.gov/paleo/taylor/taylor.html) and SI data for fossil *B. pendula* and *B. pubescens* from Lake Lille Gribsø, Denmark (right curve; see Table 1). The arrows indicate accelerator mass spectrometry ^{14}C chronologies used for temporal control (Table 1). The shaded time interval corresponds to the 8.2-ka-B.P. cooling event (3–12). Quantification of mean CO_2 concentrations is based on the rate of historical CO_2 responsiveness of the European tree birches (Fig. 1); ±1σ CO_2 estimates are derived from the standard deviation of the SI mean values.

levels >300 ppmv after ≈300 years. Timing and duration of the century-scale CO_2 excursion are in harmony with the proxy records for the 8.2-ka-B.P. cooling event embracing a period of 200–300 years between ≈8,400 and ≈8,100 years B.P. (3–12). The SI signals thus indicate a temporal association between the 8.2-ka-B.P. cooling and atmospheric CO_2 concentration. The exact phase relationship between changes in temperature and CO_2 cannot be determined yet.

Our CO_2 reconstructions reflect rapid changes with a significantly greater magnitude than the smooth and modest atmospheric CO_2 decline to values ≈260 ppmv inferred from the low-resolution Taylor Dome ice-core record (Fig. 2). The data also confirm the regular occurrence of early Holocene atmospheric CO_2 concentrations well above 300 ppmv, unknown from Antarctic ice cores but common in leaf-based time series (9, 14). These apparent controversies between leaf-based and ice-based CO_2 data have not been resolved yet (ref. 35; see text at www.sciencemag.org/cgi/content/full/286/5446/1815a). It should be noted that early Holocene records from Greenland ice cores have repeatedly indicated rapidly fluctuating CO_2 levels including values >300 ppmv (36, 37). At present, the Antarctic record is usually considered to be reliable, so that discrepancies are ascribed to CO_2 enrichment within the Greenland ice (38, 39). However, there is evidence that in polar ice also postdepositional CO_2 depletion could occur, but underlying chemical processes of this potential source of error have not yet been investigated in detail (38, 39).

The documented coupling between CO_2 fluctuations and the 8.2-ka-B.P. cooling implies a distinctive involvement of the oceans, where short-term perturbations of sea-surface temperature and/or salinity allow rapid CO_2 transfer between the atmosphere and surface waters. Holocene cooling events are generally related to a reduction in the thermohaline circulation, resulting in sea-surface temperature lowering in large parts of the North Atlantic (3, 6). This forcing mechanism is evident particularly for the 8.2-ka-B.P. cooling event, where weakening of the thermohaline circulation was triggered by catastrophic release of Laurentide meltwater (12). By applying a freshwater perturbation over 20 years, a global atmosphere-sea-ice-ocean model simulation of the 8.2-ka-B.P. event produces a 320-year lasting weakening of the North Atlantic thermohaline circulation and 1–5°C surface cooling over the adjacent continents (40).

The reconstructed atmospheric CO_2 reduction of ≈25 ppmv indicates a temporarily enhanced North Atlantic sink for CO_2 at the time of the 8.2-ka-B.P. cooling event. While regional palynological data support temperature changes (11), vegetation reconstructions do not provide evidence of an extended terrestrial sink. The occurrence of global CO_2 fluctuations substantiates the interpretation of $\delta^{18}O$ records in ice cores from Antarctica and Greenland in terms of globally parallel climate changes on the Northern and Southern Hemispheres (41). The CO_2 fluctuations falsify conclusively the concept of an approximate antiphase relation between short-term temperature changes on the two hemispheres that would cause buffering of North Atlantic CO_2 drawdown by the effects of synchronous sea-surface temperature increase in the Southern Ocean (42). It thus may be concluded that leaf-based CO_2 data support a much more dynamic evolution of the Holocene CO_2 regime than previously thought. In effect, there seems to be every indication that the occurrence of Holocene CO_2 fluctuations is more consistent with current observations and models of past global temperature changes than the common notion of a relatively stable CO_2 regime until the onset of the Industrial Revolution.

We thank Frans Bunnik, David Dilcher, Morten Fischer-Mortensen, Lenny Kouwenberg, Wolfram Kürschner, Jette Raal-Hanssen, David Robinson, Bas van Geel, Tom van Hoof, and two anonymous reviewers for constructive comments and stimulating discussions on the topic. This work was supported by the Danish Research Councils and the Council for Earth and Life Sciences of the Netherlands Organization for Scientific Research. This paper is Netherlands Research School of Sedimentary Geology publication no. 20020602.

1. Etheridge, D. M., Steele, L. P., Langenfels, R. L., Barnola, J. M. & Morgan, V. I. (1996) *J. Geophys. Res. D 2* **101,** 4115–4128.
2. Indermühle, A., Stocker, T. F., Joos, F., Fischer, H., Smith, H. J., Wahlen, M., Seck, B., Mastroianni, D., Tschumi, J., Blunier, T., *et al.* (1999) *Nature (London)* **398,** 121–126.
3. Bond, G., Showers, W., Cheseby, M., Lotti, R., Almasi, P., DeMenocal, P., Priore, P., Cullen, H., Hajdas, I. & Bonani, G. (1997) *Science* **278,** 1257–1266.
4. Alley, R. B., Mayewski, P. A., Sowers, T., Stuiver, M., Taylor, K. C. & Clark, P. U. (1997) *Geology* **25,** 483–486.
5. Walker, M. J. C., Björck, S., Lowe, J. J., Cwynar, L. C., Johnsen, S., Knudsen, K. L., Wolfarth, B. & INTIMATE Group (1999) *Quat. Sci. Rev.* **18,** 1143–1150.
6. DeMenocal, P., Ortiz, J., Guilderson, T. & Sarnthein, M. (2000) *Science* **288,** 2198–2202.
7. Von Grafenstein, U., Erlenkeuser, H., Müller, J., Jouzel, J. & Johnsen, S. (1998) *Clim. Dyn.* **14,** 73–81.
8. Klitgaard-Kristensen, D., Sejrup, H. P., Haflidason, H., Johnsen, S. & Spurk, M. (1998) *J. Quat. Sci.* **13,** 165–169.
9. Willemse, N. W. & Törnquist, T. E. (1999) *Geology* **27,** 580–584.
10. McDermott, F., Mattey, D. P. & Hawkesworth, C. (2001) *Science* **294,** 1328–1331.
11. Tinner, W. & Lotter, A. F. (2001) *Geology* **29,** 551–554.
12. Barber, D. C., Dyke, A., Hillaire-Marcel, C., Jennings, A. E., Andrews, J. T., Kerwin, M. W., Bilodeau, G., McNeely, R., Southon, J., Morehead, M. D. & Gagnon, J. M. (1999) *Nature (London)* **400,** 344–348.
13. Rundgren, M. & Beerling, D. J. (1999) *Holocene* **9,** 509–513.
14. Wagner, F., Bohncke, S. J. P., Dilcher, D. L., Kürschner, W. M., Van Geel, B. & Visscher, H. (1999) *Science* **284,** 1971–1973.
15. McElwain, J. C., Mayle, F. E. & Beerling, D. J. (2002) *J. Quat. Sci.* **17,** 21–29.
16. Woodward, F. I. (1987) *Nature (London)* **327,** 617–618.
17. Wagner, F., Below, R., De Klerk, P., Dilcher, D. L., Joosten, H., Kürschner, W. M. & Visscher, H. (1996) *Proc. Natl. Acad. Sci. USA* **93,** 11705–11708.
18. Kürschner, W. M., Wagner, F., Visscher, E. H. & Visscher, H. (1997) *Geol. Rundsch.* **86,** 512–517.
19. Gray, J. E., Holroyd, G. H., Van der Lee, F., Sijmons, P. C., Woodward, F. I., Schuch, W. & Hetherington, A. M. (2000) *Nature (London)* **408,** 713–715.
20. Beerling, D. J., Birks, H. H. & Woodward, F. I. (1995) *J. Quat. Sci.* **10,** 379–384.
21. Van de Water, P. K., Leavitt, S. W. & Betancourt, J. L. (1994) *Science* **264,** 239–242.
22. Van der Burgh, J., Visscher, H., Dilcher, D. L. & Kürschner, W. M. (1993) *Science* **260,** 1788–1790.
23. Royer, D. L., Wing, S. L., Beerling, D. J., Jolley, D. W., Koch, P. L., Hickey L. J. & Berner, R. A. (2001) *Science* **292,** 2310–2313.
24. Kürschner, W. M., Wagner, F., Dilcher, D. L. & Visscher, H. (2001) in *Geological Perspectives of Global Climate Change*, eds. Gerhard, L. C., Harrison, W. E. & Hanson, B. M. (Am. Assoc. Petroleum Geologists, Tulsa, OK), pp. 155–175.
25. Retallack, G. J. (2001) *Nature (London)* **411,** 287–290.
26. Björck, S., Kromer, B., Johnsen, S., Bennike, O., Hammarlund, D., Lemdahl, G., Possnert, G., Rasmussen, T. L., Wolfarth, B., Hammer, C. U. & Spurk, M. (1996) *Science* **274,** 1155–1160.
27. Monnin, E., Indermühle, A., Dällenbach, A., Flückiger, J., Stauffer, B., Stocker, T. F., Raynaud, D. & Barnola, J.-M. (2001) *Science* **291,** 112–114.
28. Poole, I. & Kürschner, W. M. (1999) in *Fossil Plants and Spores: Modern Techniques*, eds. Jones, T. P. & Rowe, N. P. (Geol. Soc., London), pp. 257–260.
29. Royer, D. L. (2001) *Rev. Palaeobot. Palynol.* **114,** 1–28.
30. Wagner, F. (1998) *The Influence of Environment on the Stomatal Frequency in Betula* (LPP Foundation, Utrecht, The Netherlands).
31. Wagner, F., Neuvonen, S., Kürschner, W. M. & Visscher, H. (2000) *Plant Ecol.* **148,** 61–69.
32. Osborne, C. (1991) *Int. Statist. Rev.* **59,** 309–336.
33. Birks, H. J. B. (1995) in *Statistical Modelling of Quaternary Environmental Data: Technical Guide*, eds. Maddy, D. & Brew J. S. (Quaternary Res. Assoc., Cambridge, U.K.), Vol. 5, pp. 161–254.
34. Ter Braak, C. J. F. (1995) *Biometrics* **41,** 859–873.
35. Indermühle, A., Stauffer, B., Stocker, T. F., Raynaud, D., Barnola, J. M., Birks, H. H., Eide, W., Birks, H. J. B., Wagner, F., Kürschner, W. M., *et al.* (1999) *Science* **286,** 1815a.
36. Oeschger, H., Beer, J., Siegenthaler, U., Stauffer, B., Dansgaard, W. & Langway, C. C. (1984) *Geophys. Monogr. Am. Geophys. Union* **29,** 299–306.

37. Smith, H. J., Wahlen, M., Mastroianni, D. & Taylor, K. C. (1997) *Geophys. Res. Lett.* **24,** 1–4.
38. Stauffer, B. & Tschumi, J. (2000) in *Physics of Ice Core Records*, ed. Hondoh, T. (Hokkaido Univ. Press, Sapporo), pp. 217–241.
39. Anklin, R. B., Barnola, J.-M., Schwander, J., Stauffer, B. & Raynaud, D. (1995) *Tellus B* **47,** 461–470.
40. Renssen, H., Goosse, H., Fichefet, T. & Campin, J. M. (2001) *Geophys. Res. Lett.* **28,** 1567–1570.
41. Grootes, P. M., Steig, E. J., Stuiver, M., Waddington, E. D. & Morse, D. L. (2001) *Quat. Res.* **56,** 289–298.
42. Raynaud, D., Barnola, J. M., Chappelaz, T., Blunier, T., Indermühle, A. & Stauffer, B. (2000) *Quat. Sci. Rev.* **19,** 9–17.